Improving the cellular invasion into PHEMA sponges by incorporation of the RGD peptide ligand: the use of copolymerization as a means to functionalize PHEMA sponges

Stefan M. Paterson,[a] Audra M. A. Shadforth,[b] Jeremy A. Shaw,[c] David H. Brown,[a,d] Traian V. Chirila,[b,e-g] Murray V. Baker[a,b]

[a] School of Chemistry and Biochemistry, M313, The University of Western Australia, Crawley, W.A. 6009, Australia

[b] Queensland Eye Institute, 41 Annerley Road, South Brisbane, Queensland 4101, Australia,

[c] Centre for Microscopy, Characterisation and Analysis, The University of Western Australia, Crawley, WA 6009, Australia

[d] Nanochemistry Research Institute, Department of Chemistry, Curtin University, Kent St, Bentley, W.A. 6102, Australia

[e] Faculty of Science and Engineering, Queensland University of Technology, Brisbane, Queensland 4001, Australia

[f] Australian Institute for Bioengineering and Nanotechnology, The University of Queensland, St Lucia, Queensland 4072, Australia

[g] Faculty of Health Sciences, The University of Queensland, Herston, Queensland 4006, Australia

ABSTRACT

A monomer that contained the RGD ligand motif was synthesized and copolymerized with 2-hydroxyethyl methacrylate using polymerization-induced phase separation methods to form poly(2-hydroxyethyl methacrylate)-based hydrogel sponges. The sponges had morphologies of aggregated polymer droplets and interconnected pores, the pores having dimensions in the order of 10 μm typical of PHEMA sponges. RGD-containing moieties appeared to be evenly distributed through the polymer droplets. Compared to PHEMA sponges that were not functionalized with RGD, the new sponges containing RGD allowed greater invasion by human corneal epithelial cells, by advancing the attachment of cells to the surface of the polymer droplets.

Keywords: PHEMA, Sponges, Peptide ligands, Cell invasion

INTRODUCTION

Tissue engineering aims at developing truly functional substitutes able to compensate for tissue loss or to restore failed organs. Although there are many strategies that can be used in tissue engineering, the use of porous polymeric scaffolds to guide the growth of cells into functioning tissue has become prominent.[1-6] Of the many different polymers available to construct tissue engineering scaffolds, those based on poly(2-hydroxyethyl methacrylate) (PHEMA) sponges have received considerable attention.[7-11] PHEMA sponges are biocompatible, macroporous, and have shown to be suitable for tissue engineering applications.[8] In addition, the synthesis of PHEMA sponges is a simple, benign, one-step procedure involving polymerization-induced phase separation, and characteristics such as porosity can easily be controlled by use of appropriate polymerization formulations.[7,8,12] In contrast to the straightforward situation for PHEMA, fabrication of other sponges used for tissue engineering has typically been achieved using methods involving toxic solvents, or via more complex methods, such as solvent casting and particulate leaching, melt moulding, freeze-drying techniques, membrane lamination, extrusion,

electrospinning and gas foaming.[13] The potential advantages of PHEMA have been further enhanced by recent findings that PHEMA – a polymer that is not normally biodegradable – can be rendered biodegradable by incorporation of peptide-based crosslinking agents, and this opens further possibilities for the use of PHEMA-based materials in tissue engineering applications.[14,15]

One drawback of PHEMA materials, including sponges, is that the hydroxyl-rich surface of PHEMA renders itself non-adhesive for living cells.[16] This characteristic appears to be a potential problem for applications where PHEMA sponges are to be used as tissue engineering scaffolds, since the scaffolds that offer poor cell adhesion are expected to experience poor cellular invasion. The lack of adhesivity to cells in polymeric materials can somewhat be overcome by incorporation of and/or functionalization with structural motifs that can promote cell adhesion, such as carboxyl[17] and sulfonyl groups.[18] However, functionalization does not always result in increased cell adhesion as motifs that make one surface more adhesive might make another type of surface less adhesive. For example, the ability of cells to adhere to polystyrene was increased when the polystyrene was functionalized with hydroxyl groups,[17] but the ability of cells to adhere to the same culture dishes decreased when the dishes were functionalized with hydroxyl-rich PHEMA.[16] Adsorption of extra cellular matrix (ECM) proteins to the surface of a scaffold is an alternative to functionalizing the scaffold with simple chemical motifs. ECM proteins can provide sequences of amino acids that serve as binding sites for integrins, trans-membrane proteins that mediate attachment of cells to the surrounding tissue, and can thus promote adhesion of cells to the scaffold.[19] However, use of ECM proteins to promote cell adhesion requires that the proteins first be purified, and can be further complicated by the occurrence of inflammation and infection, undesirable immune response, and issues of protein denaturation masking the integrin-binding sites.[19]

The short amino acid sequences from the ECM proteins involved in binding to the cell's integrin sites are known as cell adhesion ligands. These short peptides can be synthesized in the laboratory, and it has been shown that incorporation of synthetic cell adhesion ligands onto the surfaces of polymers greatly increases cell adhesion.[19-22] The first cell adhesion ligand to be reported

was the Arg-Gly-Asp (RGD) peptide sequence,[23] which is the integrin binding site of fibronectin, laminin, vitronectin, type I collagen and other ECM proteins.[19] Most research into cell adhesion ligands has focused on flat two-dimensional surfaces,[24-28] but reports of functionalization of porous three-dimensional scaffolds with cell adhesion ligands have recently emerged.[29-31] Kubinová *et al*. demonstrated[29] that super-porous PHEMA scaffolds could be functionalized with the laminin-derived IKVAV (Ile-Lys-Val-Ala-Val) adhesion ligand, which resulted in increased cell adhesion. However, the functionalization was a multi-step process, involving copolymerization of amine-based monomers, functionalizing the amine group with primary thiol groups post-polymerization, and finally conjugating the IKVAV peptide to the thiol; each step requiring washings with organic solvents.[29]

To simplify the functionalization procedure, it would be advantageous to incorporate RGD ligands into the polymer network by copolymerization, thereby eliminating additional synthetic steps. Copolymerization has been investigated by Hejčl *et al*.[30] as a method to functionalize poly(N-(2-hydroxypropyl)methacrylamide) (PHPMA) scaffolds with RGD moieties. Like PHEMA scaffolds, PHPMA scaffolds can be prepared via a procedure involving polymerization-induced phase separation, but unlike PHEMA, PHPMA requires the use of solvents that are toxic to cells, and extensive post-polymerisation washing procedures were required to remove those solvents before the PHPMA scaffolds could be used. The PHPMA scaffolds were used for *in vivo* neural regeneration studies, and it was found that the presence of RGD increased cell adhesion and improved neural regeneration. Despite the simplicity of copolymerization as a method to incorporate RGD-containing motifs into scaffolds, there are, to the best of our knowledge, few reports that detail its use for preparation of PHEMA sponges functionalized with RGD motifs. Therefore, the aim of this investigation was to carry out proof-of-concept experiments to demonstrate the potential for use of copolymerization in water as a method to produce PHEMA sponges functionalized with RGD motifs via polymerization-induced phase separation methods. To determine the effectiveness of copolymerization, this study examined the synthesis of RGD-

containing monomers, the distribution of RGD motifs within the polymer scaffold, and the effect of RGD functionalization on the adhesion of human corneal epithelial cells to the scaffold.

EXPERIMENTAL

Materials

2-Hydroxyethyl methacrylate (HEMA) (min. 99%, from Bimax, USA) was distilled (b.p. 38–39 °C/0.1 mm Hg) and stored at -20 °C until use. Tetraethyleneglycol dimethacrylate (TEGDMA) (Fluka/Sigma-Aldrich, USA) and 2,2-dimethoxy-2-phenylacetophenone (DPAP) (Irgacure 651) (97%, from Aldrich) were used as received. The syntheses of **1** and methacryloyl N-hydroxysuccinimide (MA-NHS) are described in the Supporting Information. Sterile ethanol (70%) was supplied by Orion Laboratories, Australia. Dulbecco's phosphate buffered saline solution (DPBS) without Ca and Mg, Hank's buffered salt solution (HBSS) with Ca and Mg, the 1:1 mixture of Dulbecco's modified Eagle's medium (DMEM) and Nutrient Mixture F12 with Glutamax™ (DMEM/F12), and the Antibiotic/Antimycotic supplement were all supplied by Invitrogen Life Technologies, Australia. Foetal bovine serum (FBS) was supplied by HyClone® Thermo Scientific, USA. Triton X-100 and HEPES were supplied by Sigma, USA, and the nuclear stain Hoechst 33342 was supplied by Invitrogen Molecular Probes, Australia. Neutral buffered formalin solution (3.7%) and Mayer's haematoxylin solution were supplied by United Biosciences, Australia. The Iwaki™ tissue culture plastic (TCP) plates (6 wells) were supplied by Asahi Glass Co., Japan.

Synthesis of the RGD containing monomer 2

Triethylamine (50 μL, 0.35 mmol) was added dropwise to a solution of the heptapeptide RGD **1** (60.1 mg, 74.9 μmol) and MA-NHS (13 mg, 74.9 μmol) in 1:2 H_2O:DMF (4.5 mL) at 0 °C. The solution was allowed to warm to room temperature and additional MA-NHS was added (26 mg, 150 μmol), and the solution was stirred for a further 3 h. The solution was concentrated *in vacuo* to approximately 0.5 mL, and diluted with approximately 3 mL of methanol, then diethyl ether was

added until a white precipitate formed. The precipitate was collected *via* centrifugation, triturated with diethyl ether and dried under vacuum. The solid was dissolved in H_2O (600 μL), and the solution was filtered through a 0.45 μm Teflon syringe filter (Phenomenex, USA) and eluted through a preparative-HPLC column (250 mm x 10 mm, Aqua 5 μm C18 125 Å; Phenomenex, USA) using an isocratic elution solvent system (10:90 A:B. A: 0.1 v./v.% TFA:CH_3CN, B: 0.1 v./v.% TFA:H_2O). The fractions containing **2** were collected, concentrated and lyophilized, to afford the trifluoroacetic acid salt of **2** (**2**.TFA) as a white solid (30.2 mg, 56%) that was stored under an inert atmosphere in a freezer. RP-HPLC (1:99 A:B to 15:85 A:B over 30 min, A: 0.1 v./v.% TFA:CH_3CN, B: 0.1 v./v.% TFA:H_2O) indicated the product was of high purity.

^{1}H NMR (600.13 MHz, d_6-DMSO, ppm): 8.21 – 8.16 (4H, m, NH^{α} Asp, NH^{ε} Arg, NH Gly × 2), 8.11 (1H, apparent t, slitting 5.7 Hz, NH Gly), 8.06 (1H, apparent t, splitting 5.7 Hz, NH Gly), 7.98 (1H, d, $^3J_{HH}$ 8.0 Hz, NH^{α} Arg), 7.46 (1H, apparent t, splitting 5.6 Hz, NH Gly), 7.40 - 6.55 (4H, m, NH^{ω} × 2, OH × 2), 5.75 (1H, s, C(CH3)=C*H*H), 5.38 (1H, m, C(CH3)=CH*H*), 4.54 (1H, apparent q, splitting 7.8 Hz, 6.38 Hz, CH^{α} Asp), 4.29 (1H, apparent dd, splitting 13.7 Hz, 7.9 Hz, CH^{α} Arg), 3.74 (10H, m, CH_2 Gly), 3.08 (2H, apparent q, splitting 6.5 Hz, CH_2^{δ} Arg), 2.68 (1H, dd, $^2J_{HH}$ 16.7 Hz, $^3J_{HH}$ 5.7 Hz, CH_2^{β} Asp), 2.59 (1H, dd, $^2J_{HH}$ 16.6 Hz, $^3J_{HH}$ 6.8 Hz, CH_2^{β} Asp), 1.87 (3H, s, C(C*H3*)=CH), 1.76-1.45 (4H, m, $CH_2^{\beta}CH_2^{\gamma}$ Arg).

^{13}C NMR (150.9 MH, d_6-DMSO, ppm) 172.2 (C=O), 171.6 (C=O), 171.4 (C=O), 169.5 (C=O), 169.4 (C=O), 167.1 (C=O), 168.8 (C=O), 168.4 (C=O), 167.8 (C=O), 158.2 (CF_3*C*=O), 156.6 (N-(*C*=N)-N Arg), 139.3 (*C*(CH_3)=CH_2), 119.8 (C(*C*H_3)=CH_2), 116.8 (*C*F_3C=O), 52.1 (CH^{α} Arg), 48.6 (CH^{α} Asp), 42.4 (CH_2 Gly), 42.0 (CH_2 Gly), 41.9 (CH_2 Gly), 41.5 (CH_2 Gly), 40.3 (CH_2 Gly), 40.0 (CH_2^{δ} Arg), 36.0 (CH^{β} Asp), 29.1 (CH_2^{β} Arg), 24.9 (CH_2^{γ} Arg), 18.5 (C(*C*H_3)=CH_2).

HRMS (FAB) m/z 643.2805 $[M+H]^+$ ($C_{24}H_{39}N_{10}O_{11}$ requires 643.2800)

Synthesis of PHEMA sponges containing RGD.

Polymer hydrogels were prepared as described previously[12] by photoinitiated polymerization of HEMA. Briefly, an 80:20 w/w H_2O:HEMA solution containing (all percentages with respect to HEMA) 1 mol % TEGDMA, 2 mol% **2**.TFA and 0.1 mol% DPAP (as an initiator), was irradiated using a UV lamp (UVP Blak-Ray®, 365 nm, 120 W) for 30 min. Control sponges were synthesized without **2**. After polymerization, the hydrogels were soaked in water for one week to remove any unreacted monomers, with water being exchanged daily.

Characterization of polymer morphologies

Polymer samples were cut into 300-μm thick cross-sections (Vibratome 3000), which were further cut into disks using a 5-mm biopsy cutter. Specimens were then frozen at -20 °C and freeze-dried (FD2, Dynavac, Hingham, Massachusetts, USA.) until a constant mass was reached. Dried samples were mounted on double-sided carbon tabs and coated with a layer of carbon (approximately 30 nm thick) using a carbon evaporator (Speedivac 12E6/1178, Edwards High Vacuum Ltd, Crawley, UK). The samples were then imaged by SEM (Zeiss 1555 VP-FESEM, Berlin, Germany) at 3 kV, using a working distance of 6 mm and an aperture of 10 μm. To acquire an image, frame integration was used to prevent charging on the surface of the polymer.

EFTEM

The distribution of **2** within polymer droplets was determined using energy filtered transmission electron microscopy (EFTEM). Hydrated RGD-functionalized PHEMA sponges were freeze-dried and ground into a fine powder using an agate mortar and pestle. Approximately 1 mg of the powder was mixed with approximately 200 μL of epoxy resin (Procure-Araldite, Proscitech, Australia) and poured into a Beem® embedding capsule (Proscitech, Australia). The epoxy resin was then polymerized by heating the resin-containing embedding capsule at 70 °C for 24 h. The resin blocks

were then cut into 150-nm thick sections using an ultramicrotome (EMC6, Leica, Vienna, Austria). The sections were then mounted on a carbon-coated copper grid. For EFTEM imaging, the mounted specimens were analyzed at 200 kV using a TEM (JEOL, Japan) fitted with a Gatan Imaging Filter (GIF, Tridiem, USA). EFTEM jump-ratio maps[32] were generated by acquiring an image at the nitrogen signal energy (411 eV signal plus background) and dividing this by a second image taken of the background (389 eV background only), each with a slit width of 20 μm. To minimize the effects of plural inelastic scattering, section thickness maps were obtained to ensure t/λ values were <1. To obtain suitable signal-to-noise levels, a 4× binning was used.

Cellular invasion assay

The effect on cell adhesion of incorporating RGD in the hydrogel substratum was investigated qualitatively using human corneal epithelial cells immortalized with SV40 (line HCE-T; source: Riken Cell Bank, Tsukuba, Japan).

The sponge specimens (as disks of approximately 7-8 mm in diameter and 2-mm thick) were sterilized overnight in sterile ethanol (70%), then washed thoroughly and soaked in DPBS. Prior to the assay, the sponges were washed in HBSS and DMEM/F12. The disks were fitted tightly within the tubes of 8-mm stainless steel surgical trephines (henceforth 'tubes') that had been sterilized in an autoclave. The tubes containing sponge disks were laid horizontally at the bottom of a well in a 6-well TCP plate, where they were completely immersed with DMEM/F12 supplemented with 10% FBS and 1% Antibiotic/Antimycotic. After 4 h, the tubes were raised to a vertical position and each was placed on a circular Teflon® stage in which a rectangular slot was cut out to allow the basal perfusion of the sponge during incubation. The medium above each sponge in the apical area of the tube was removed and fresh medium was added. The HCE-T cells were seeded at a density of 20,000 cells/cm^2 in the apical area of the tubes and also in several wells devoid of sponge samples (positive controls on TCP). The levels of medium inside the tube and in the well outside were brought to the same height. Cultures were incubated at 37 ºC in 5% CO_2 for 14 days. The medium

in the apical area was replaced after one day with fresh medium, while the medium surrounding the tube was refreshed on day 5 and day 8. On day 14, the cultures were fixed in neutral buffered formalin solution (3.7%). The sponges were removed from the tubes, washed with DPBS, dehydrated and infiltrated with paraffin. The samples were cut lengthwise in half before being embedded into paraffin blocks. Sections were cut, mounted on slides, deparaffinized, and either stained with Mayer's haematoxylin or permeabilized with 0.1% Triton X-100 in 100 mM HEPES buffer and stained with the nuclear stain Hoechst 33342. Bright field and fluorescence microscopy (Nikon TE2000-U, Japan) was used to visualize and photograph the nuclei.

RESULTS AND DISCUSSION

Synthesis of the RGD-containing monomer

It is generally accepted that to ensure accessibility to the RGD ligand, it is best to include a spacer group between the RGD sequence and the polymer surface.[19] There is debate in the literature as to what length this spacer group should be,[19] but it has been shown that a GGGG spacer group is sufficiently long to allow correct binding between the RGD motif and integrins on the cell surface.[24] With these ideas in mind, we synthesized the sequence GGGG-RGD, **1** (Scheme 1).Functionalisation of the N-terminus of **1** with a methacryloyl group using N-hydroxysuccinimide-activated methacrylic acid (MA-NHS) in 1:2 H_2O:DMF with triethylamine as the base gave the methacryloyl-GGGG-RGD, **2**. The monomer **2** was purified by preparative HPLC (Figure 1A) and isolated as its trifluoroacetic acid salt, **2**.TFA. The presence of the polymerizable methacryloyl group in **2** was confirmed by the observation signals for the vinylic protons at 6.0 – 5.0 ppm in the ^{1}H NMR spectrum (Figure 1B). The monomer **2** is similar to the monomer methacryloyl-GG-RGD, which was incorporated into hydroxypropyl methacrylate hydrogels used in an experimental treatment of spinal chord injury.[30] While we appreciate that there are more active cell adhesion ligands, such as the cyclic RGDfK sequence,[19] the use of RGD contained in **2** served

as a simple proof-of-concept cell adhesion ligand for assessing the usefulness of copolymerization as a means to functionalize PHEMA sponges with such ligands.

Formation and characterization of RGD-functionalized PHEMA sponges

The RGD-containing monomer **2** was copolymerized with HEMA in 80:20 H_2O:HEMA to give RGD-functionalized PHEMA sponges. The sponges had an internal morphology comprised of agglomerated polymer droplets of 3 to 5 μm in diameter and pores with dimensions in the order of 20 μm (Figure 2), which is typical of 80:20 PHEMA sponge formulations.[7,12] As RGD can only promote cell growth if it is located at the surface of the polymer droplets, the distribution of **2** within polymer droplets was examined. Since **2** was the only component of the polymer that contained nitrogen, energy filtered transmission electron microscopy (EFTEM) could be used to explore the nitrogen distribution in the polymer droplets, and, therefore, the distribution of RGD from **2** that has been incorporated into the polymer network. Figure 3A shows a micrograph (without elemental mapping) of a polymer droplet with a diameter of *ca*. 5 μm; the dark diagonal area extending through the white polymer droplet in Figure 3A is an artefact (folding of the sample) introduced during specimen sectioning. When EFTEM was used to detect nitrogen on the same sample (Figure 3B), it revealed an even distribution of nitrogen throughout the polymer droplet. Although the nitrogen distribution was apparently uniform on the micron scale, it is possible that nitrogen is buried many nanometres below the surface of droplets and hence inaccessible to cells. Intuitively, however, it could be argued that even if such a distribution existed, the chains in a hydrogel should be mobile enough to diffuse to the surface and present RGD groups to cells.

Cellular invasion of sponges

Due to the irregularities in shape and morphology of the sponge specimens, we considered that cell counts determined from microscope images are not reliable quantitative indicators of cell adhesion, and consequently only a qualitative assessment was carried out. The cells spread in significant

numbers along the surface of the RGD-containing sponges. There were clear signs of a cellular invasion into the sponges (Figure 4 A, B), also confirmed by the localization of cells' nuclei as revealed by specific staining (Figure 4 C, D). In the PHEMA sponges that do not contain RGD, however, the cells clumped together, forming clusters adjacent to the surface of the sponge (Figure 5 A) or in occasional crevices (Figure 5 B), with only minor (if any) attachment to the PHEMA substrate and without spreading further. There was no sign of cells invading into the pores of the RGD-free PHEMA sponges, as indicated also by the localization of nuclei (Figure 5 C, D). The patterns seen in Figure 4 for RGD-PHEMA were seen consistently on all RGD-PHEMA samples examined, and similarly the patterns seen in Figure 5 for RGD-free PHEMA were seen consistently on all other samples of RGD-free PHEMA that were examined. These results indicate that the presence of RGD improves cellular infiltration into PHEMA-based sponges, presumably by providing integrin binding motifs to which the cells may adhere. However, other factors apart from the presence of RGD should be considered when investigating when cellular infiltration and attachment. For example, it is known that the presence of RGD alone is not always sufficient to assure cell-adhesive properties on substratum.[19] So, while the presence of RGD may not be sole reason for improved cellular infiltration into PHEMA sponges – surface topography and surface chemistry, for example, could also affect cellular infiltration – these results demonstrate the potential for copolymerization as a method to incorporate RGD-containing monomers and that further investigations are warranted to ascertain the mechanisms behind cellular infiltration in PHEMA sponges functionalized with RGD motifs.

CONCLUSIONS

This proof-of-concept investigation demonstrates the use of copolymerization as a means to incorporate RGD-containing moieties into PHEMA-based sponges, using polymerization-induced phase separation methods. The RGD peptide ligand motif can be incorporated covalently into PHEMA by copolymerization of HEMA with a monomer containing this RGD moiety. The RGD-

containing PHEMA sponges obtained by the polymerization-induced phase separation exhibit typical droplet morphology (polymer droplets and large interconnected pores), and the RGD moieties are distributed uniformly throughout the polymer network. Although the common PHEMA sponges are not invaded in vitro by human corneal epithelial cells, the RGD-containing PHEMA sponges allow invasion by the advancing attachment of cells to the internal walls of the pores. Despite the promising results, further investigations are required to define in detail the processes involved in RGD-mediated cellular infiltration in PHEMA sponges that contain RGD motifs.

ACKNOWLEDGEMENTS

The authors thank the Australian Research Council for financial support (to M.V.B., T.V.C.) and an Australian Postgraduate Award (to S.M.P.), and Curtin University of Technology for a Research and Teaching Fellowship (to D.H.B.). We acknowledge the Australian Microscopy and Microanalysis Research Facility at the Centre of Microscopy, Characterisation and Analysis, The University of Western Australia (a facility funded by The University of Western Australia, the Australian Government and the State Government of Western Australia) for providing access to facilities, and for scientific and technical assistance.

SUPPORTING INFORMATION

Full details for synthesis and characterization of the RGD-containing sequence. This material is available free of charge via the Internet at XXXXXXXXXX

REFERENCES

(1) Langer, R.; Vacanti, J. *Science* **1993,** 260, 920-926.

(2) Vacanti, J. P.; Morse, M. A.; Saltzman, W. M.; Domb, A. J.; Perez-Atayde, A.; Langer, R. *J. Pediat. Surg.* **1988,** 23, 3-9.

(3) Cima, L. G.; Vacanti, J. P.; Vacanti, C.; Ingbar, D.; Mooney, D.; Langer, R. *J. Biomech. Eng.* **1991,** 113, 143-151.

(4) Corckhill, P. H.; Fitton, J. H.; Tighe, B. J. *J. Biomat. Sci. Polym. Ed.* **1993,** 4, 6150-6630.

(5) Silva, A. I.; Norton de Matos, A.; Brons, G. I.; Mateus, M. *Med. Res. Rev.* **2006,** 26, 181-222.

(6) Methcalfe, A. D.; Ferguson, M. W. J. *Biomaterials* **2007,** 28, 5100-5113.

(7) Chirila, T. V.; Chen, Y.-C.; Griffin, B. J.; Constable, I. J. *Polym. Int.* **1993,** 32, 221-232.

(8) Chirila, T. V.; Constable, I. J.; Crawford, G. J.; Vijayasekaran, S.; Thompson, D. E.; Chen, Y.-C.; Flethcher, W. A.; Griffin, B. J. *Biomaterials* **1993,** 14, 26-38.

(9) Plant, G. W.; Harvey, A. R.; Chirila, T. V. *Brain Res.* **1995,** 671, 119-130.

(10) Plant, G. W.; Chirila, T. V.; Harvey, A. R. *Cell Transplant.* **1998,** 7, 381-391.

(11) Hicks, C. R.; Morris, I. T.; Vijayasekaran, S.; Fallon, M. J.; McAllister, J.; Clayton, A. B.; Chirila, T. V.; Crawford, G. J.; Constable, I. J. *Br. J. Ophthalmol.* **1999,** 83, 616-621.

(12) Baker, M. V.; Brown, D. H.; Casadio, Y. S.; Chirila, T. V. *Polymer* **2009,** 50, 5918-5927.

(13) Murphy, M. B.; Mikos, A.G.; *Polymer scaffold fabrication*. In: Lanza, R.; Langer, R.; Vacanti, J. (eds). *Principles of tissue engineering*. Amsterdam: Elsevier; 2007. p. 309–21.

(14) Khelfallah, N. S.; Decher, G.; Mésini, P. J. *Macromol. Rapid Comm.* **2006,** 27, 1004-1008.

(15) Casadio, Y. S.; Brown, D. H.; Chirila, T. V.; Kraatz, H.-B.; Baker, M. V. *Biomacromolecules* **2010,** 11, 2949-2959.

(16) Lydon, M. J.; Minett, T. W.; Tighe, B. J. *Biomaterials* **1985,** 6, 396-402.

(17) Curtis, A. S. G.; Forrester, J. V.; Mcinnes, C.; Lawrie, F. *J. Cell Biol.* **1983,** 97, 1500-1506.

(18) Kowalczynska, H. M.; Kaminski, J. *J. Cell Sci.* **1991,** 99, 587-593.

(19) Hersel, U.; Dahmen, C.; Kessler, H. *Biomaterials* **2003,** 24, 4385-4415.

(20) Hubbell, J. A.; Massia, S. P.; Drumheller, P. D. *Ann. N.Y. Acad. Sci.* **1992,** 665, 253-258.

(21) Schamberger, P. C.; Gardella Jr., J. A. *Colloid. Surfaces B* **1994,** 2, 209-223.

(22) Sakiyama-Elbert, S.; Hubbell, J. *Annu. Rev. Mater. Res.* **2001,** 31, 183-201.

(23) Pierschbacher, M. D.; Rouslahti, E. *Nature* **1984,** 309, 30-33.

(24) Lee, J. W.; Park, Y. J.; Lee, S. J.; Lee, S. K.; Lee, K. Y. *Biomaterials* **2010,** 31, 5545-5551.

(25) Tugulu, S.; Silacci, P.; Stergiopulos, N.; Klok, H.-A. *Biomaterials* **2007,** 28, 2536-2546.

(26) Kantlehner, M.; Schaffner, P.; Finsinger, D.; Meyer, J.; Jonczyk, A.; Diedenbach, B.; Nies, B.; Holzemann, G.; Goodman, S. l.; Kessler, H. *Chem. Biol. Chem.* **2000,** 1, 107-114.

(27) Hern, D. L.; Hubbell, J. A. *J. Biomed. Mater. Res. A* **1998,** 39, 266-276.

(28) Beer, J. H.; Springer, K. T.; Coller, B. S. *Blood* **1992,** 79, 117-128.

(29) Kubinová, S.; Horák, D.; Kozubenko, N.; Vanecek, V.; Proks, V.; Price, J.; Cocks, G.; Syková, E. *Biomaterials* **2010,** 31, 5966-75.

(30) Hejčl, A.; Sedý, J.; Kapcalová, M.; Toro, D. A.; Amemori, T.; Lesný, P.; Likavcanová-Mašínová, K.; Krumbholcová, E.; Prádný, M.; Michálek, J.; Burian, M.; Hájek, M.; Jendelová, P.; Syková, E. *Stem Cells Dev.* **2010,** 19, 1535-46.

(31) Blit, P. H.; Shen, Y. H.; Ernsting, M. J.; Woodhouse, K. A.; Santerre, J. P. *J. Biomed. Mater. Res.* **2010,** 94A, 1226-1235.

(32) Brydson, R., *Electron Energy Loss Spectroscopy*. 1st ed., vol. 1; BIOS Scientific Publishers Limited: Oxford, 2001.

Figure and Scheme Captions

Scheme 1. Synthesis of the RGD-containing monomer **2**.

Figure 1. Characterization of the RGD-containing monomer **2**, using (A) RP-HPLC and (B) ^{1}H NMR spectroscopy (d_6-DMSO).

Figure 2. An SEM image of an RGD-functionalized PHEMA sponge.

Figure 3. (A) A TEM micrograph showing a polymer droplet from an RGD-functionalized PHEMA sponge, and (B) an EFTEM jump-ratio image showing the distribution of nitrogen for the sample specimen. Brighter regions in (B) correspond to regions with higher nitrogen content than darker regions. The dark diagonal lines in (A) and (B) are artefacts (folding of the sample) introduced during sample preparation prior to EFTEM analysis.

Figure 4. Cell cultures in the presence of the RGD-containing PHEMA sponge. The microphotographs were taken in a Nikon TE2000-U microscope in either conventional or fluorescence mode. A, B: Cells penetrating into the material; C, D: The same cultures with the cells' nuclei stained. The scale bar is the same for all panels.

Figure 5. Behavior of cells in the presence of a PHEMA sponge that does not contain RGD peptide. The microphotographs were taken in a Nikon TE2000-U microscope in either conventional (A, B) or fluorescence (C, D) mode. A: Cells growing adjacent to the sponge but not spreading or penetrating further; B: Cells clumping inside a large crevice but not penetrating the pores; C, D: The same cultures with the cells' nuclei stained. The scale bar is the same for all panels.

Scheme 1

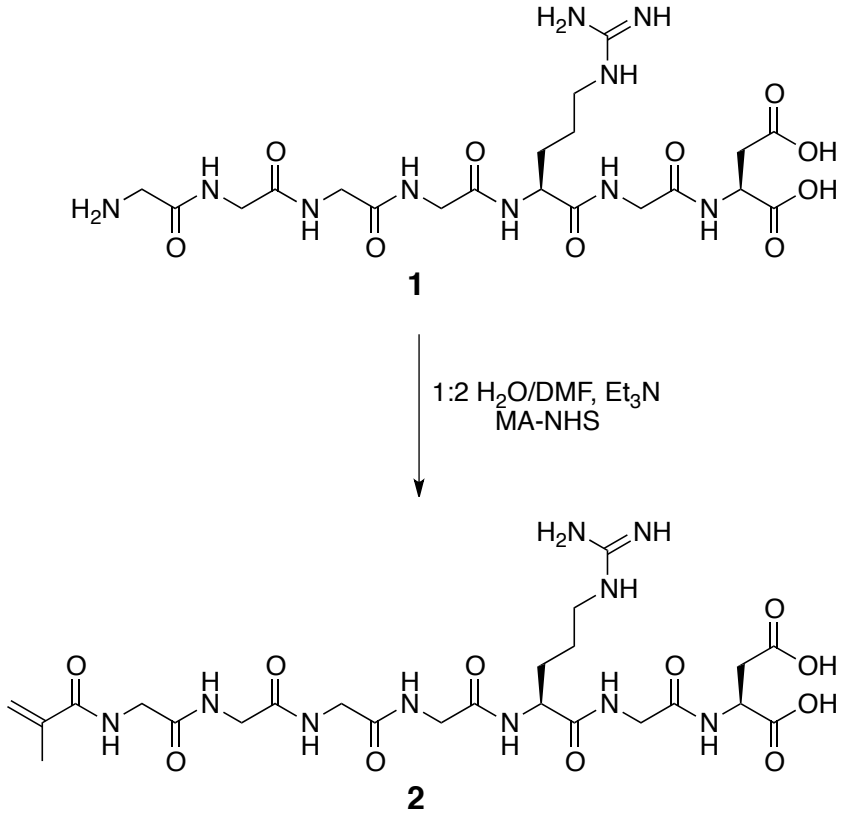

Fig. 1

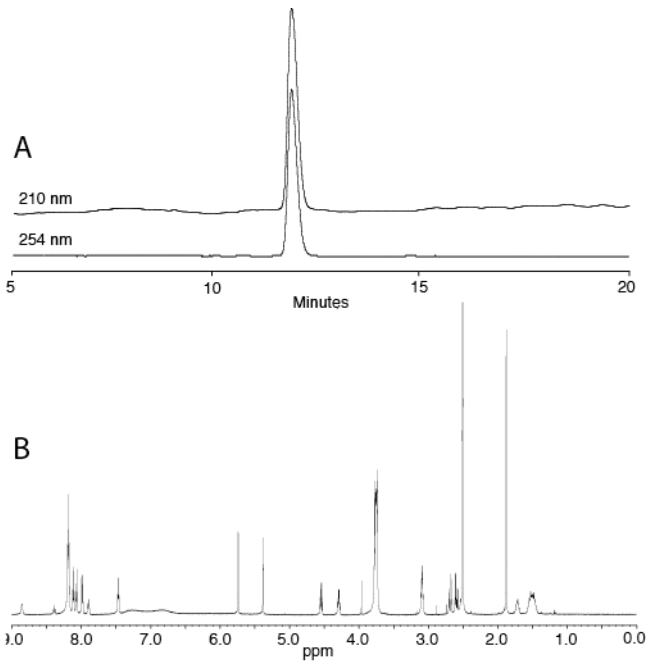

Fig. 2

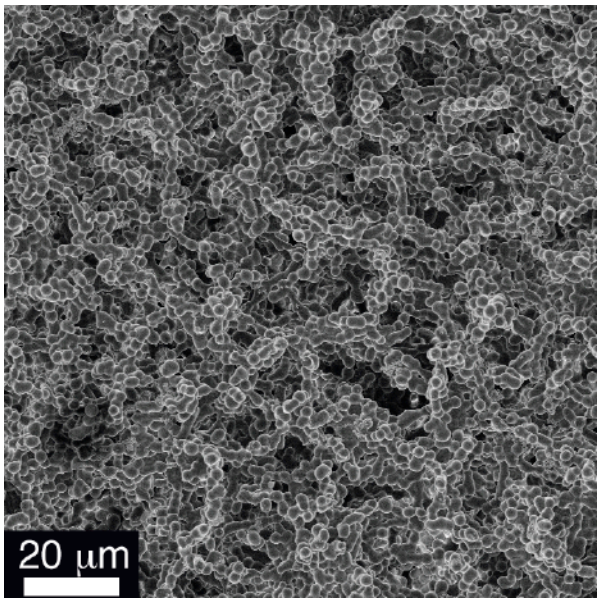

Fig. 3

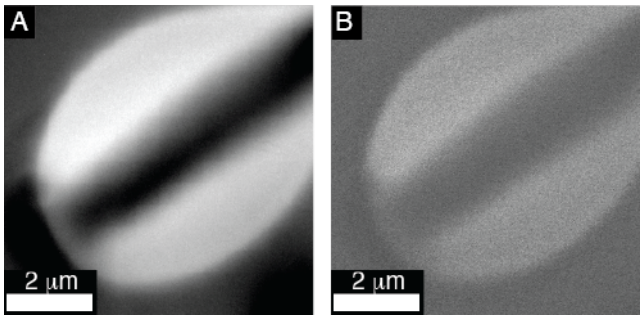

Fig. 4

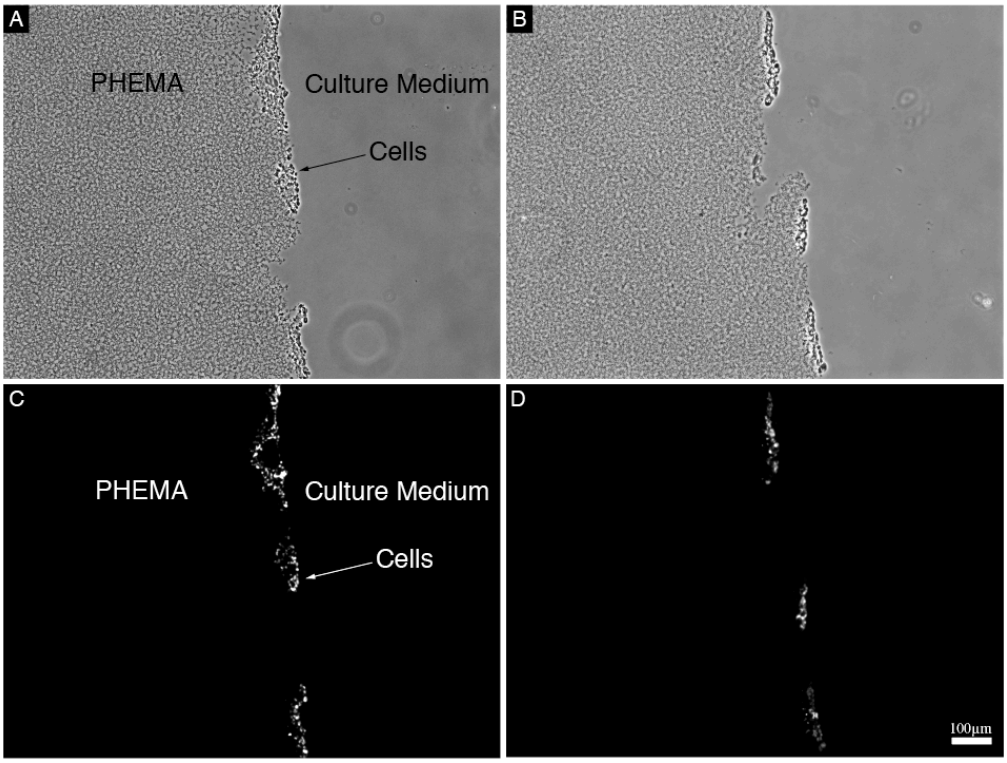
A
PHEMA
Culture Medium
Cells
B
C
PHEMA
Culture Medium
Cells
D
100μm

Fig. 5

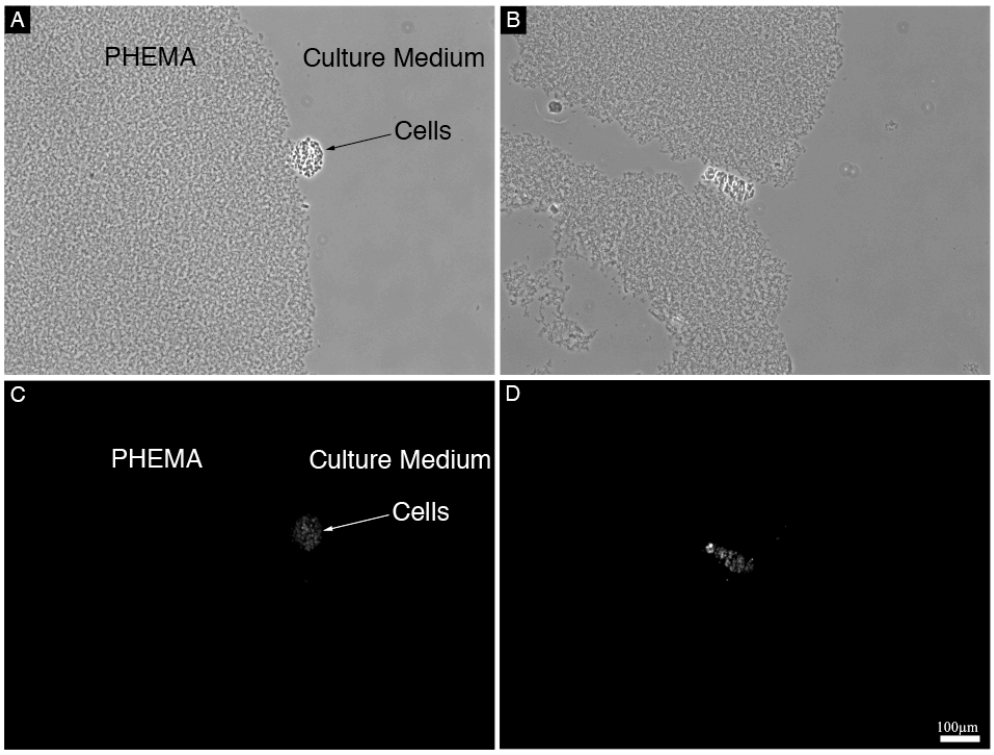
A
PHEMA
Culture Medium
Cells
B
C
PHEMA
Culture Medium
Cells
D
100μm